

Sea Spray Aerosol Structure and Composition Using Cryogenic Transmission Electron Microscopy

Joseph P. Patterson,^{*,†} Douglas B. Collins,[†] Jennifer M. Michaud,[†] Jessica L. Axson,[†] Camile M. Sultana,[†] Trevor Moser,[‡] Abigail C. Dommer,[†] Jack Conner,[†] Vicki H. Grassian,[§] M. Dale Stokes,^{||} Grant B. Deane,^{||} James E. Evans,[‡] Michael D. Burkart,[†] Kimberly A. Prather,^{†,||} and Nathan C. Gianneschi[†]

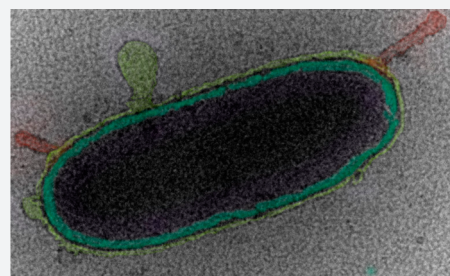
[†]Department of Chemistry & Biochemistry and ^{||}Scripps Institution of Oceanography, University of California, San Diego, La Jolla, California 92093, United States

[‡]Environmental Molecular Science Laboratory, Pacific Northwest National Laboratory, 3335 Innovation Boulevard, Richland, Washington 99354, United States

[§]Department of Chemistry, University of Iowa, Iowa City, Iowa 52242, United States

S Supporting Information

ABSTRACT: The composition and surface properties of atmospheric aerosol particles largely control their impact on climate by affecting their ability to uptake water, react heterogeneously, and nucleate ice in clouds. However, in the vacuum of a conventional electron microscope, the native surface and internal structure often undergo physicochemical rearrangement resulting in surfaces that are quite different from their atmospheric configurations. Herein, we report the development of cryogenic transmission electron microscopy where laboratory generated sea spray aerosol particles are flash frozen in their native state with iterative and controlled thermal and/or pressure exposures and then probed by electron microscopy. This unique approach allows for the detection of not only mixed salts, but also soft materials including whole hydrated bacteria, diatoms, virus particles, marine vesicles, as well as gel networks within hydrated salt droplets—all of which will have distinct biological, chemical, and physical processes. We anticipate this method will open up a new avenue of analysis for aerosol particles, not only for ocean-derived aerosols, but for those produced from other sources where there is interest in the transfer of organic or biological species from the biosphere to the atmosphere.



INTRODUCTION

Our understanding of how complex atmospheric aerosols are impacting clouds and climate will depend on our ability to obtain detailed information on aerosol three-dimensional (3D) structure, morphology, and composition under controlled and variable environmental conditions. Electron microscopy (EM) has provided insight into both aerosol structure and composition, taking advantage of high spatial resolution, elemental analysis capabilities via energy dispersive X-ray spectroscopy, and 3D imaging using electron tomography.¹ However, native structures are difficult to study with EM due to the high vacuum requirements of the microscope, which are known to affect particle structure, particularly hydrated or soft matter.² For particles in solution, cryogenic transmission electron microscopy (cryo-TEM) has revolutionized the study of dynamic, soft, and biological particles,^{2,3} through the use of cryofixation, whereby the solution is cooled at a rate of 10^4 to 10^6 K per second resulting in a liquid to solid phase transition, fast enough to avoid any organization of the water molecules and consequently resulting in the trapping of amorphous ice.^{3a,4} Consequently, we hypothesized that this same approach could be applied to trap the native or nascent structure of aerosol particles. Therefore, we report the first cryo-TEM experiments

of hydrated aerosol particles demonstrating the power and utility of this technique through the study of laboratory generated sea spray aerosols (SSA).

SSA are generated through wave action and bubble bursting at the air–sea interface⁵ and have been shown to be highly complex systems consisting of both sea salt and organic components. To date, dry-state electron microscopy has led to the conclusion that these important environmental nanoparticles are phase separated.⁶ Thorough investigation of particle size, morphology, phase separation, and composition is considered critical because these properties will profoundly influence their behavior and the climate through their ability to serve as seeds upon which liquid and ice clouds form and to directly scatter solar radiation.⁷ In contrast to previous analyses, our observations by cryo-TEM reveal previously undetected phases of SSA, yield unprecedented images of biological structures inside SSA particles, and show that without cryogenic methods, significant reorganization of SSA morphology is observed when samples are aged under laboratory conditions or exposed to high vacuum in conventional EM. Conventionally,

Received: October 19, 2015

Published: January 15, 2016

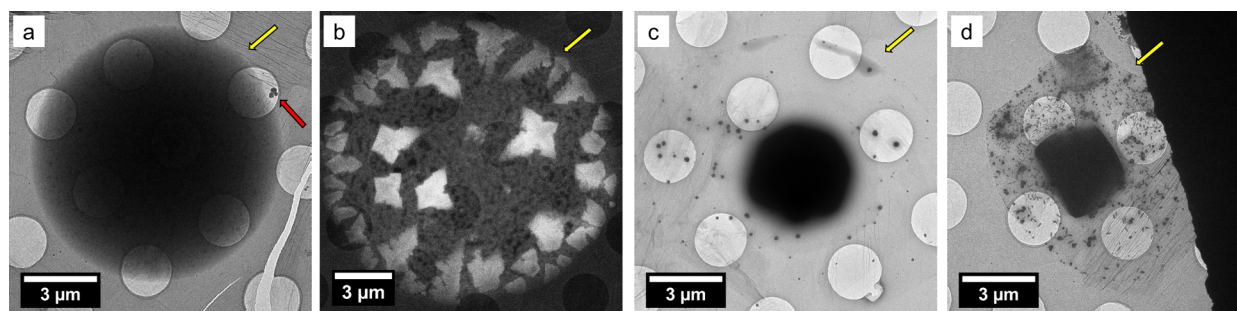


Figure 1. (S)TEM images representative of $>1 \mu\text{m}$ particles collected after different stages of reorganization. (a) TEM image at stage 1, nascent SSA, (b) HADDF STEM image at stage 2, efflorescence, (c) TEM image at stage 3, after laboratory drying and aging (note: the large salt crystal appears out of focus as it is too thick to image through), and (d) TEM image at stage 4 after exposure to high vacuum. Yellow arrows indicate the edge of the SSA, and the red arrow indicates contamination from the cryo-TEM preparation.

SSA particle analysis by EM has been conducted by collection of particles either in liquid form using an impinger—whereby aerosols are collected into an aqueous medium (which can later be applied to a TEM grid),⁸ or via direct impaction onto TEM grids,^{6b,9} using, for example, a micro-orifice uniform-deposit impactor (MOUDI) for size separation.^{6a} In previous studies, there has been no mention of, and indeed little attention paid to, particle aging time or storage conditions before insertion into the electron microscope,^{9,10} at which point they are exposed to high vacuum conditions. Freedman et al have explored the use of cold holders to reduce aerosol damage under the electron beam.¹¹ However, in this study, samples were inserted into the microscope at room temperature, and then exposed to a vacuum.^{11,12} There have been several reports of aerosols being imaged using environmental scanning electron microscopy (E-SEM) and environmental transmission electron microscopy (E-TEM), which allow for particles to be imaged under hydrated conditions. However, the conditions are representative only of water saturated conditions and not a natural representation of a liquid environment. Furthermore, prior to imaging, particle aging and exposure to high vacuum occur,^{9b,13} which, as we have discovered in this work, prevents the imaging of nascent SSA.

RESULTS AND DISCUSSION

SSA Generation and Collection. Several stages of reorganization can occur following the generation of nascent SSA before they are imaged, including depositions onto a substrate (stage 1), dehydration and efflorescence (stage 2), particle drying and aging under laboratory conditions (stage 3), and exposure to vacuum upon insertion into the microscope (stage 4). To date, particles have been imaged by EM at stage 4, after drying and aging under laboratory conditions and exposure to high vacuum; consequently we lack a thorough investigation of the transformations that occur prior to these stages and the ability to trap the nascent hydrated structure of SSA. While it is currently impossible to image an airborne particle inside an electron microscope, we hypothesized that by using cryo-TEM it would be possible to investigate the sequential stages of reorganization within a few seconds of deposition onto a substrate and trap the hydrated structure of the particles, which in this paper we consider to be nascent SSA. In this study, SSA was generated using state-of-the-art laboratory production mechanisms using a wave channel¹⁴ and marine aerosol reference tanks (MART).¹⁵ However, the techniques presented here could readily be applied to those collected in field studies. Furthermore, the SSA generated by

MART and wave channel systems have been shown to be representative of those formed from breaking waves in the open ocean,¹⁵ over a wide size and range of compositions. SSA is produced from natural seawater, collected from the surface ocean at Scripps Pier ($32^\circ 52.0' \text{ N}$, $117^\circ 15.4' \text{ W}$) approximately 275 m from shore. Figure 1 shows S/TEM images for SSA generated from natural sea water using a MART and processed according to procedures laid out in the Supporting Information. Briefly, aerosols are passively adhered to either graphene oxide (GO_x) or carbon coated TEM grids (used only for the images in Figure S9),¹⁶ vitrified by plunging into either liquid ethane or nitrogen, and kept at $< -170^\circ \text{C}$ while being inserted into the microscope and during imaging. Control samples were collected by placing the grids inside the wave channel or the MART in the absence of the wave breaking mechanism, thereby negating SSA production; images are shown in Figure S1. TEM and STEM Images were recorded on either an FEI Titan operating at 300 keV with spherical aberration corrected TEM and STEM with a Si(Li) X-ray energy dispersive spectrometer (EDS) or an FEI Sphera microscope operated at 200 keV. Low dose imaging procedures were used in order to prevent beam damage to the particles. Sommerdijk and co-workers have described in detail the artifacts and image interpretation associated with cryo-TEM images;^{3a} here, we will indicate SSA particles with a blue arrow, biological structures with a green arrow and contamination with a red arrow. Imaging SSA by cryo-TEM presents certain challenges; in particular, for SSA particles $\gg 1 \mu\text{m}$, there were often very thin as well as very thick regions within the sample particle. Consequently, a variety of imaging conditions, e.g., bright field TEM, bright field STEM, and high angle annular dark field (HADDF) STEM, were used in order to obtain the relevant information for each particle; the specific imaging conditions is noted in the figure caption for each image.

SSA: Nascent Structure, Efflorescence and Aging. The images in Figure 1 are representative cryo-(S)TEM or TEM images collected from multiple grids where >50 particles were imaged in each case, and the images are representative of the general morphology observed in each case; additional images are provided in the Supporting Information. Vitrification of SSA at stage (1) (Figure 1a, Figure S2) shows wet aerosol droplets adhered to the grid. No phase separation was observed, and energy dispersive X-ray spectroscopy (EDS) showed a similar Na/Mg ratio when measuring at both the center and the edge of the particle. (Figure S3). The particles shown were trapped as quickly as 30 s after production, so these represent images of truly nascent SSA after deposition

onto a substrate. Droplets with diameters between 100 nm and 20 μm were observed. However, as prepared GO_x is significantly hydrophilic and has been shown to give water contact angles of ca. 12° ,¹⁷ this means a significant wetting of the surface will occur, flattening out the particle. Furthermore, using the electron energy loss spectroscopy (EELS) log-ratio method for thickness measurements,¹⁸ we estimate that the center of 15–20 μm particles has a rough liquid thickness of 550 nm, which indicates that the wet aerosol diameter was around a factor of 6 smaller than the measured TEM diameter. Given these considerations, we estimate a particle diameter range of 20 nm to 10 μm in this study. For larger particles, this spreading is extremely beneficial in order to create liquid layers thin enough to achieve high resolution imaging. However, it has been observed that substrate hydrophobicity is extremely important for some aerosol measurements (e.g., water uptake properties).¹⁹ When necessary, the hydrophobicity of the GO_x -TEM grids can be tuned accordingly.¹⁷ After adherence to the grid, if SSA particles are subjected to low relative humidity (ca. RH = 20%) laboratory conditions for 30–60 s before vitrification, the initial stages of particle dehydration and efflorescence can be observed by cryo-TEM (stage 2, Figure 1b and Figure S4). Here, we observe an early stage of salt crystallization where dendrites appear to form on the particle surface. Indeed, in other work, a similar “nonspatially homogeneous” efflorescence was also observed for ammonium sulfate water aerosols with glutaric acid, by surface aerosol microscopy.²⁰ EDS analysis of the particle type in Figure 1b reveals the dendrites are rich in Na and that there is a distinct lack of Na present in the center of the aerosol (Figure S5). The 3D interpretation of this information is that during the initial stages of dehydration, NaCl begins to crystallize at the particle surface, leaving a Na depleted particle core. Na, Mg phase separation has been previously reported for SSA and shown to be affected when SSA undergo reactions with nitric acid at 60% RH;^{6a} therefore, cryo-TEM could provide key insights into the mechanism of these surface active processes. If these particles are not subjected to vitrification prior to insertion into the microscope, significant structural reorganization occurs upon exposure to a vacuum, which typically results in Na-rich salt crystals surrounded by a ring of particle residue. This was observed when warming the cryo-TEM samples to room temperature within the microscope, which itself results in little deformation of the particles. However, removal from the microscope after warming, followed by reinsertion (after 2 min) at room temperature causes significant rearrangement (Figure S6). Therefore, cryo-TEM is essential for imaging the hydrated surface structure of SSA, which is of paramount importance to understanding their impact on the environment. If particles are allowed to age on the grid (ca. 3 h, ambient laboratory conditions) prior to vitrification (stage 3, Figure 1c and Figure S7), their structure appears similar to those which are not vitrified before imaging and subjected to high vacuum (HV) (stage 4, Figure 2d and Figure S8). Here, it can be seen that $>1 \mu\text{m}$ particles typically contain a large salt crystal, which is occasionally surrounded by a residue of mixed organic/salt species, similar to previous observations.^{6a,c,10} A similar experiment was performed on hydrophobic amorphous carbon TEM grids, and again similar results were obtained, inducing the observation of small dendrite salt crystals on the particle surface and a reorganization after aging or exposure to high vacuum (Figure S9). However, it was noted qualitatively that fewer particles adhered to the hydrophobic grids and that

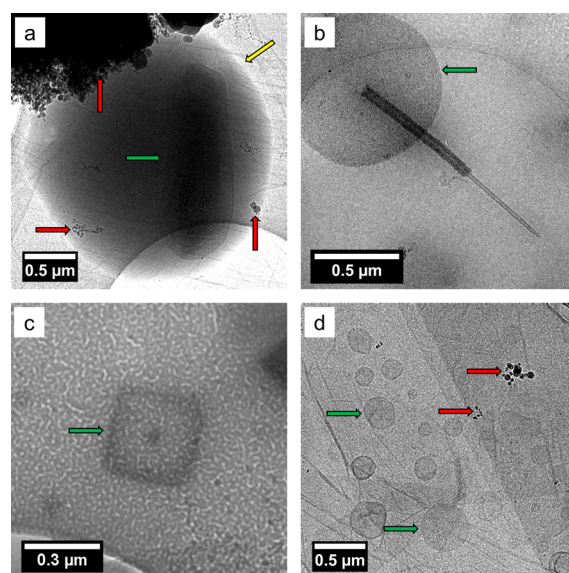


Figure 2. Bright field TEM images of SSA prepared by cryo-TEM showing (a) a whole bacterium inside a wet SSA droplet (note: the image contrast and brightness was adjusted to aid the observation of the cell, the original image is shown in Figure S11), (b) an intact diatom, (c) a virus particle, and (d) marine membrane vesicles. The biological structures were identified according to their size, shape, and morphology (see Supporting Information for more details). Yellow arrows indicate the edge of the SSA, the red arrows indicate contamination from the cryo-TEM preparation, and the green arrows indicate the biological particles.

particles of a similar diameter appeared to be high contrast on the carbon grids (indicating they were thicker and less spread out), both of which are consistent with GO_x being hydrophilic.^{16a,17} Efflorescence is an extremely important phenomenon in atmospheric science,²¹ and therefore the ability to trap particles during the first efflorescent event after aerosol production can provide unique insights. While there have been numerous investigations into particle efflorescence by electron microscopy,^{9b,22} these studies have only examined SSA efflorescence after particles have been created, dehydrated, and then rehydrated, rather than the very first efflorescence event. Substrate deposited SSA storage (over weeks or months) and imaging methods have recently been investigated,²³ and it was concluded that ambient imaging conditions provide the most relevant particle size measurement. Here, we trap the ambient structure by vitrification, and use this process to investigate aging over short time periods (minutes to seconds) and by exposure to high vacuum. We have shown that the phase and organization of salt crystals in SSA can be greatly affected by exposure to HV (Figure 1 and Figure S6). Work is ongoing in our lab to fully utilize cryo-TEM in order to study efflorescence for a range of complex aerosol particle compositions.

Biological Structures in SSA. Next we sought to investigate the morphology and composition of nascent SSA by cryo-TEM as a function of biologically mediated changes in seawater chemical composition.²⁴ This was achieved through the addition of Guillard’s f/2 growth medium plus sodium metasilicate and continuous illumination (5700 K fluorescent lamps; $\sim 100 \mu\text{E m}^{-2} \text{s}^{-2}$), to induce a phytoplankton bloom, in both the MART and wave flume. Over the course of the bloom, many biological structures were observed inside wet SSA particles (Figure 2), including whole bacteria (Figure 2a), diatoms (Figure 2b), viruses (Figure 2c), and membrane

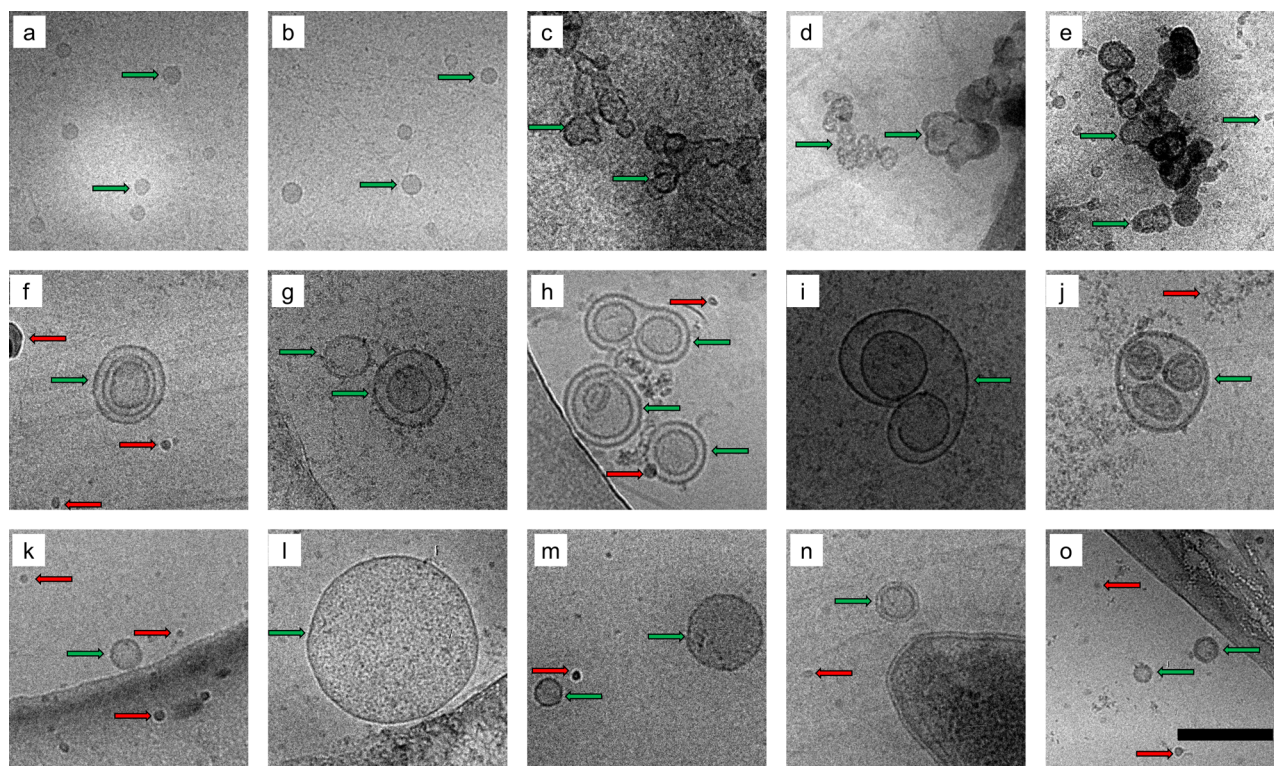


Figure 3. Bright field TEM images of membrane vesicles from aerosols (top row, a–e), SSML (middle row f–j) and bulk (bottom row, k–o) blue, were collected from a MART experiment during a phytoplankton bloom. Scale bar = 200 nm. The red arrows indicate contamination from the cryo-TEM preparation, and the green arrows indicate the membrane vesicles.

vesicles (Figure 2d). Importantly, these images demonstrate that cryo-TEM can be used to preserve soft biological structures within SSA, as well as provide direct evidence that whole intact biological structures and cells can be ejected into the atmosphere in hydrated form (i.e., in a salt containing sea spray aerosol particle). Biological particles have been detected previously in SSA.^{6b,c,9a,10,25} However, with conventional TEM it is impossible to probe the hydrated nature of the SSA droplets within which they exist. In addition, the vacuum of the microscope induces changes to their delicate structures,² which makes distinguishing between different types of biological particles (e.g., vesicles, marine nanogels, bacteria cells) extremely difficult. Therefore, our observations suggest that cryo-TEM has the potential to be used to characterize particles harboring hydrated life forms from one aqueous environment to another while traveling over significant distances as hydrated aerosols.^{7d} It should be noted that while Raman, optical, and atomic force microscopy techniques can all be performed at ambient pressure and high relative humidity, the trapping of particles by vitrification prevents any further reorganization or aging of the particles allowing the structure of nascent sea spray to be captured. Furthermore, cryo-TEM has significantly higher spatial resolution than Raman or optical microscopy, allowing the nanoparticles within SSA particles to be easily identified, and in comparison to AFM, cryo-TEM allows the imaging of particle internal structure.

Membrane Vesicles in SSA. Recently Chisholm et al. showed, by concentration and purification of large volumes (ca. 90 L) of bulk seawater, that membrane vesicles make up a small but significant component of the oceanic loading of colloidal particles with diameter (d) < 200 nm.²⁶ Furthermore, their production by *Prochlorococcus* (a marine cyanobacterium) was

observed from large-scale lab cultures, allowing the presence of DNA, RNA, and proteins within the membrane vesicles to be confirmed.²⁶ These nanometer-scale vehicles act as concentrating containers for biological species and chemical information in the ocean, but hitherto have never been detected before this study in the aerosol phase. This is likely due to the reorganization that occurs within noncryogenic imaging techniques, thereby obscuring or destroying the soft nanostructures. Figure 3 shows cryo-TEM images for membrane vesicles collected from the aerosol (Figure 3a–e), the sea surface microlayer (SSML) (Figure 3f–j), and the bulk seawater (Figure 3k–o), revealing the structural variability and complexity of these vesicles. Chisholm et al. reported an increase in vesicle concentration with decreasing depth in the ocean from 10^4 (500 m depth) to 10^6 (surface).²⁶ Here, we show similar concentrations for bulk surface seawater (approximately 0.5 m depth) and approximately a 3-fold increase for the SSML, (ca. 10^7 vesicles mL^{-1} Table S1) collected via a glass plate method, whereby glass substrates are dipped into the surface of the water and removed in order to capture the top hydrophobic layer onto the glass substrate. Furthermore, we find a remarkably high fraction (20%) of complex multilamellar vesicles (MLVs) in the SSML when compared to the bulk, where a low fraction of MLVs (<5%) were observed. The structural differences between membrane vesicles observed in aerosols (Figure 3a–e), which are more aggregated or have a narrower size distribution (Figure S5) compared to the SSML/bulk samples (Figure 3f–o), indicate that these vesicles might not simply be ejected as intact structures like bacteria shown in Figure 2a. We contend that rather than being ejected as already intact structures from seawater, we propose that the shear forces associated with

bubble bursting at the surface promote self-assembly of these structures in the lipid-salt matrix.²⁷ Vesicles could conceivably influence aqueous phase reactivity by providing an interface within the hydrated droplet or act as a container for larger biomolecules, which would influence their availability at the gas-particle interface. Indeed, the formation of membrane vesicles in aerosols has previously been proposed by Dobson et al. as an important step in abiogenesis.²⁸ Our observation that these types of structures can indeed be formed during aerosol production and remain stable within aerosols strongly supports this theory. The membrane vesicles in Figure 3a,b were obtained from impinged solutions collected at the same time as particles shown in the images in Figure 3c–e collected as aerosols by cryo-TEM. The obvious structural differences between particles seen in Figure 3a,b, which show discrete uniform vesicles versus particles seen in Figure 3c–e, which show disperse aggregated vesicles, indicate a further rearrangement upon re-entry into a dilute continuous liquid phase. This result opens up many questions about which additional chemical species they contain and transfer processes at play between the ocean and the atmosphere. Membranes act as barriers for smaller biogenic species such as proteins, enzymes, and DNA. The morphology, composition, and phase state of particles have been shown to affect processes such as gas-particle mass transfer,²⁹ and gas-particle reactions,³⁰ and therefore this structural rearrangement may have profound consequences for the chemistry of the aerosol particles as they travel through the atmosphere and undergo changes in hydration, temperature, pressure, oxidation, and UV radiation exposure.

Marine Gels in SSA. Marine gels are also important biological entities for the storage and transfer of biological and organic material in the marine environment.³¹ A gel can be defined as a nonfluid colloidal network or polymer network that is expanded throughout its whole volume by a fluid.³² Therefore, direct evidence of a gel should include an observation of the network structure or physical testing of mechanical properties. Several working definitions serve as indirect evidence for marine gels, such as a spontaneous self-assembly,^{7c,31} disassembly in the presence of EDTA (which binds the divalent Ca^{2+} and Mg^{2+} metals holding the network structure together),^{7c,31} and staining with Alcian blue for acidic polysaccharides, Coomassie Blue for amino acids and chlortetracycline for Ca^{2+} ,^{7c,33} all of which are known to be components of marine gels. While there have been numerous studies on marine gels in the seawater,^{31,34} there have been very few reports of marine gels in aerosols. Orellana et al. found indirect evidence for gels in high Arctic cloudwater using chlortetracycline, EDTA disassembly, and pH responsive swelling.^{7c} Bigg and Leck have observed gel-like aggregates in aerosol particles by TEM.^{25a,b} However, the network structure was not clear, and as pointed out by Verdugo,³⁵ conventional electron microscopy is not suitable for studying these structures as it can readily lead to network-like artifacts. For cryo-TEM, the combination of low dose imaging and the trapping of hydrated particles will prevent these network-like artifacts from forming during sample preparation, thereby allowing the observation of the native network of the gels. Furthermore, it should be noted that cryo-TEM is an established method for imaging the network structure of synthetic hydrogels.³⁶ Here, we directly observe the network structure of marine gels throughout the entire volume of wet aerosol particles collected after the senescence phase of a laboratory phytoplankton bloom

(Figure 4). Under cryogenic imaging conditions (Figure 4a,b and S13a), the particles typically appear to have no significant

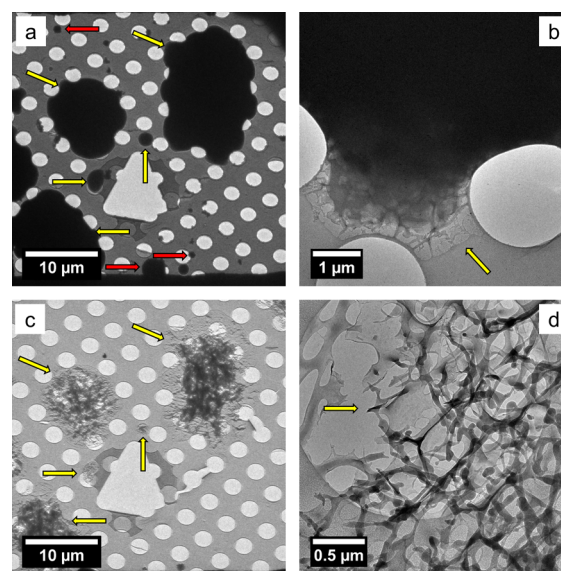


Figure 4. Bright field TEM images of gel SSA particles, (a) and (b) show hydrated particles, which are too thick to observe any internal morphology; however a network structure is observed at the edge; the particles in (b–d) show images after controlled dehydration inside the microscope, which reveals a network structure that was present throughout the entire liquid aerosol droplet. The yellow arrows indicate the edges of the SSA and the red arrow shows contamination from the cryo-TEM preparation.

phase separation; however, some network-like structures can be observed at particle edges (Figure 4b). EDS analysis for these particles shows a significant lack of Na and Mg signals when compared to the particles shown in Figure S3, indicating their salt concentration is significantly lower than for the typical SSA discussed previously. Bigg and Leck have discussed a film drop formation mechanism by which SSA particles can become significantly depleted of salts,^{6b,c} and therefore it is possible these gels were formed through such a film drop mechanism. The sample was then selectively dehydrated inside the microscope, by raising the temperature of the holder to ca. $-135\text{ }^{\circ}\text{C}$, at which point a sharp pressure increase in the microscope column was observed. Post dehydration, the network structure of the gel-type particles was revealed and shown to have been present throughout the entire the liquid aerosol droplet (Figure 4c,d) and S13c). EDS spectra recorded after dehydration (Figure S13d) shows a large decrease in the O signal, due to loss of water, and reveals the presence of weak Na, Mg, and Cl signals, which were previously obscured. This is the first observation of an SSA gel particle and shows that the network structure presents on the surface of the particle and therefore interfaces with the atmosphere, which could affect the climate-relevant properties of these aerosols.

CONCLUSIONS

Sea spray aerosol is a mixture of biological and chemical constituents that are often external mixtures of particle types. The use of cryo-TEM allows us to measure these different chemical and biological components intact for the first time leading to an unprecedented understanding of these particles and their nanostructures. Through laboratory studies, we have

demonstrated that this approach allows investigations into the chemical and morphological changes that occur when particles are exposed to various environmental (for example, changing humidity) or nonenvironmental (for example, high vacuum) conditions. For SSA, we observed that, upon ejection, most nascent SSA are essentially homogeneous water droplets, which then rapidly reorganize and phase separate upon exposure in a lower relative humidity environment. This reorganization involves the formation of NaCl dendrites on the surface of the particle as well as a phase separation of salts within the bulk of the particle. We report the first observation of marine vesicles within aerosols, which have important implications for carbon/biomolecule cycling, cloud formation, as well as the study of abiogenesis. Furthermore, we have imaged the network structure of marine gels in aerosols for the first time, showing that they can penetrate through an entire aerosol droplet. With the ability to trap aerosols under environmentally relevant hydrated conditions, studies can now begin to address many of the questions posed about the chemical complexity and structure of aerosol particles and how they impact climate and the environment for both laboratory and field studies.

■ ASSOCIATED CONTENT

Supporting Information

The Supporting Information is available free of charge on the ACS Publications website at DOI: [10.1021/acscentsci.5b00344](https://doi.org/10.1021/acscentsci.5b00344).

Additional S/TEM images, including EDS analysis, experimental information detailing the synthesis of the GO grids, aerosol production methods, and the calculations for vesicle concentration (PDF)

■ AUTHOR INFORMATION

Corresponding Author

*E-mail: jppatterson@ucsd.edu.

Notes

The authors declare no competing financial interest.

■ ACKNOWLEDGMENTS

This work was conducted within the Center for Aerosol Impacts on Climate and the Environment (CAICE), an NSF Center for Chemical Innovation and supported by the NSF (CHE-1305427). We acknowledge use of the UCSD Cryo-Electron Microscopy Facility, which is supported by NIH Grant R37 GM-03350 to Dr. Timothy S. Baker and a gift from the Agouron Institute to UCSD. A portion of the cryo-S/TEM work was performed using the Environmental Molecular Sciences Laboratory (EMSL), a national scientific user facility sponsored by the Department of Energy's Office of Biological and Environmental Research and located at PNNL.

■ REFERENCES

- (1) (a) Goodhew, P. J.; Humphreys, F. J.; Beanland, R. *Electron Microscopy and Analysis*; Taylor & Francis Group: New York, 2001. (b) Williams, D. B.; Carter, C. B. *The Transmission Electron Microscope*; Springer: Berlin, 1996.
- (2) Adrian, M.; Dubochet, J.; Lepault, J.; McDowell, A. W. Cryo-electron microscopy of viruses. *Nature* **1984**, *308* (5954), 32–36.
- (3) (a) Friedrich, H.; Frederik, P. M.; de With, G.; Sommerdijk, N. A. J. M. Imaging of Self-Assembled Structures: Interpretation of TEM and Cryo-TEM Images. *Angew. Chem., Int. Ed.* **2010**, *49* (43), 7850–7858. (b) Nudelman, F.; de With, G.; Sommerdijk, N. A. J. M. Cryo-electron tomography: 3-dimensional imaging of soft matter. *Soft Matter* **2011**, *7* (1), 17–24. (c) Newcomb, C. J.; Moyer, T. J.; Lee, S.

S.; Stupp, S. I. Advances in cryogenic transmission electron microscopy for the characterization of dynamic self-assembling nanostructures. *Current Opinion in Colloid & Curr. Opin. Colloid Interface Sci.* **2012**, *17* (6), 350–359.

(4) Almgren, M.; Edwards, K.; Karlsson, G. Cryo transmission electron microscopy of liposomes and related structures. *Colloids Surf., A* **2000**, *174* (1–2), 3–21.

(5) O'Dowd, C. D.; De Leeuw, G. Marine aerosol production: a review of the current knowledge. *Philos. Trans. R. Soc., A* **2007**, *365* (1856), 1753–1774.

(6) (a) Ault, A. P.; Guasco, T. L.; Ryder, O. S.; Baltrusaitis, J.; Cuadra-Rodriguez, L. A.; Collins, D. B.; Ruppel, M. J.; Bertram, T. H.; Prather, K. A.; Grassian, V. H. Inside versus Outside: Ion Redistribution in Nitric Acid Reacted Sea Spray Aerosol Particles as Determined by Single Particle Analysis. *J. Am. Chem. Soc.* **2013**, *135* (39), 14528–14531. (b) Bigg, E. K.; Leck, C. The composition of fragments of bubbles bursting at the ocean surface. *J. Geophys. Res.* **2008**, *113* (D11), No. D11209, DOI: [10.1029/2007JD009078](https://doi.org/10.1029/2007JD009078).

(c) Leck, C.; Bigg, E. K. Source and evolution of the marine aerosol—A new perspective. *Geophys. Res. Lett.* **2005**, *32* (19), L19803. (d) Ault, A. P.; Moffet, R. C.; Baltrusaitis, J.; Collins, D. B.; Ruppel, M. J.; Cuadra-Rodriguez, L. A.; Zhao, D.; Guasco, T. L.; Ebben, C. J.; Geiger, F. M.; Bertram, T. H.; Prather, K. A.; Grassian, V. H. Size-Dependent Changes in Sea Spray Aerosol Composition and Properties with Different Seawater Conditions. *Environ. Sci. Technol.* **2013**, *47* (11), 5603–5612. (e) Ault, A. P.; Zhao, D.; Ebben, C. J.; Tauber, M. J.; Geiger, F. M.; Prather, K. A.; Grassian, V. H. Raman microspectroscopy and vibrational sum frequency generation spectroscopy as probes of the bulk and surface compositions of size-resolved sea spray aerosol particles. *Phys. Chem. Chem. Phys.* **2013**, *15* (17), 6206–6214.

(7) (a) Schill, S. R.; Collins, D. B.; Lee, C.; Morris, H. S.; No-vak, G. A.; Prather, K. A.; Quinn, P. K.; Sultana, C. M.; Tivanski, A. V.; Zimmermann, K.; Cappa, C. D.; Bertram, T. H. The Impact of Aerosol Particle Mixing State on the Hygroscopicity of Sea Spray Aerosol. *ACS Cent. Sci.* **2015**, *1* (3), 132–141. (b) Langmann, B.; Scannell, C.; O'Dowd, C. New Directions: Organic matter contribution to marine aerosols and cloud condensation nuclei. *Atmos. Environ.* **2008**, *42* (33), 7821–7822. (c) Orellana, M. V.; Matrai, P. A.; Leck, C.; Rauschenberg, C. D.; Lee, A. M.; Coz, E. Marine microgels as a source of cloud condensation nuclei in the high Arctic. *Proc. Natl. Acad. Sci. U. S. A.* **2011**, *108* (33), 13612–13617. S13612/1-S13612/4 (d) Konstantinidis, K. T. Do airborne microbes matter for atmospheric chemistry and cloud formation? *Environ. Microbiol.* **2014**, *16* (6), 1482–1484. (e) Adler, G.; Koop, T.; Haspel, C.; Taraniuk, I.; Moise, T.; Koren, I.; Heiblum, R. H.; Rudich, Y. Formation of highly porous aerosol particles by atmospheric freeze-drying in ice clouds. *Proc. Natl. Acad. Sci. U. S. A.* **2013**, *110* (51), 20414–20419. S20414/1-S20414/10 (f) Farmer, D. K.; Cappa, C. D.; Kreidenweis, S. M. Atmospheric Processes and Their Controlling Influence on Cloud Condensation Nuclei Activity. *Chem. Rev.* **2015**, *115* (10), 4199–4217.

(8) Verreault, D.; Moineau, S.; Duchaine, C. Methods for Sampling of Airborne Viruses. *Microbiology and Molecular Biology Reviews* **2008**, *72* (3), 413–444.

(9) (a) Leck, C.; Bigg, E. K. New Particle Formation of Marine Biological Origin. *Aerosol Sci. Technol.* **2010**, *44* (7), 570–577. (b) Wise, M. E.; Freney, E. J.; Tyree, C. A.; Allen, J. O.; Martin, S. T.; Russell, L. M.; Buseck, P. R. Hygroscopic behavior and liquid-layer composition of aerosol particles generated from natural and artificial seawater. *J. Geophys. Res.* **2009**, *114* (D3), No. D03201.

(10) Bigg, E. K.; Leck, C. Properties of the aerosol over the central Arctic Ocean. *Journal of Geophysical Research: Atmospheres* **2001**, *106* (D23), 32101–32109.

(11) Veghte, D. P.; Bittner, D. R.; Freedman, M. A. Cryo-Transmission Electron Microscopy Imaging of the Morphology of Submicrometer Aerosol Containing Organic Acids and Ammonium Sulfate. *Anal. Chem.* **2014**, *86* (5), 2436–2442.

- (12) Veghte, D. P.; Altaf, M. B.; Freedman, M. A. Size De-pendence of the Structure of Organic Aerosol. *J. Am. Chem. Soc.* **2013**, *135* (43), 16046–16049.
- (13) Laskina, O.; Morris, H. S.; Grandquist, J. R.; Qin, Z.; Stone, E. A.; Tivanski, A. V.; Grassian, V. H. Size Matters in the Water Uptake and Hygroscopic Growth of Atmospherically Relevant Multicomponent Aerosol Particles. *J. Phys. Chem. A* **2015**, *119* (19), 4489–4497.
- (14) Wernand, M. R.; van der Woerd, H. J.; Gieskes, W. W. C. Trends in Ocean Colour and Chlorophyll Concentration from 1889 to 2000, Worldwide. *PLoS One* **2013**, *8* (6), e63766.
- (15) (a) Prather, K. A.; Bertram, T. H.; Grassian, V. H.; Deane, G. B.; Stokes, M. D.; DeMott, P. J.; Aluwihare, L. L.; Palenik, B. P.; Azam, F.; Seinfeld, J. H.; Moffet, R. C.; Molina, M. J.; Cappa, C. D.; Geiger, F. M.; Roberts, G. C.; Russell, L. M.; Ault, A. P.; Baltrusaitis, J.; Collins, D. B.; Corrigan, C. E.; Cuadra-Rodriguez, L. A.; Ebben, C. J.; Forestieri, S. D.; Guasco, T. L.; Hersey, S. P.; Kim, M. J.; Lambert, W. F.; Modini, R. L.; Mui, W.; Pedler, B. E.; Ruppel, M. J.; Ryder, O. S.; Schoepp, N. G.; Sullivan, R. C.; Zhao, D. Bringing the ocean into the laboratory to probe the chemical complexity of sea spray aerosol. *Proc. Natl. Acad. Sci. U. S. A.* **2013**, *110* (19), 7550–7555. S7550/1-S7550/10 (b) Stokes, M. D.; Deane, G. B.; Prather, K.; Bertram, T. H.; Ruppel, M. J.; Ryder, O. S.; Brady, J. M.; Zhao, D. A Marine Aerosol Reference Tank system as a breaking wave analogue for the production of foam and sea-spray aerosols. *Atmos. Meas. Tech.* **2013**, *6* (4), 1085–1094. (c) Collins, D. B.; Zhao, D. F.; Ruppel, M. J.; Laskina, O.; Grandquist, J. R.; Modini, R. L.; Stokes, M. D.; Russell, L. M.; Bertram, T. H.; Grassian, V. H.; Deane, G. B.; Prather, K. A. Direct aerosol chemical composition measurements to evaluate the physicochemical differences between controlled sea spray aerosol generation schemes. *Atmos. Meas. Technol. Discuss.* **2014**, *7* (7), 6457–6499.
- (16) (a) Wilson, N. R.; Pandey, P. A.; Beanland, R.; Young, R. J.; Kinloch, I. A.; Gong, L.; Liu, Z.; Suenaga, K.; Rourke, J. P.; York, S. J.; Sloan, J. Graphene Oxide: Structural Analysis and Application as a Highly Transparent Support for Electron Microscopy. *ACS Nano* **2009**, *3* (9), 2547–2556. (b) Pantelic, R. S.; Meyer, J. C.; Kaiser, U.; Baumeister, W.; Plitzko, J. M. Graphene oxide: A substrate for optimizing preparations of frozen-hydrated samples. *J. Struct. Biol.* **2010**, *170* (1), 152–156. (c) van de Put, M. W. P.; Patterson, J. P.; Bomans, P. H. H.; Wilson, N. R.; Friedrich, H.; van Benthem, R. A. T. M.; de With, G.; O'Reilly, R. K.; Sommerdijk, N. A. J. M. Graphene oxide single sheets as substrates for high resolution cryoTEM. *Soft Matter* **2015**, *11*, 1265–1270.
- (17) Patterson, J. P.; Sanchez, A. M.; Petzetakis, N.; Smart, T. P.; Epps, T. H., III; Portman, I.; Wilson, N. R.; O'Reilly, R. K. A simple approach to characterizing block copolymer assemblies: graphene oxide supports for high contrast multi-technique imaging. *Soft Matter* **2012**, *8* (12), 3322–3328.
- (18) Malis, T.; Cheng, S. C.; Egerton, R. F. EELS log-ratio technique for specimen-thickness measurement in the TEM. *J. Electron Microsc. Tech.* **1988**, *8* (2), 193–200.
- (19) Eom, H.-J.; Gupta, D.; Li, X.; Jung, H.-J.; Kim, H.; Ro, C.-U. Influence of Collecting Substrates on the Characterization of Hygroscopic Properties of Inorganic Aerosol Particles. *Anal. Chem.* **2014**, *86* (5), 2648–2656.
- (20) Peckhaus, A.; Grass, S.; Treuel, L.; Zellner, R. Deliquescence and Efflorescence Behavior of Ternary Inorganic/Organic/Water Aerosol Particles. *J. Phys. Chem. A* **2012**, *116* (24), 6199–6210.
- (21) (a) Martin, S. T. Phase Transitions of Aqueous Atmospheric Particles. *Chem. Rev. (Washington, DC, U. S.)* **2000**, *100* (9), 3403–3453. (b) Onasch, T. B.; Siefert, R. L.; Brooks, S. D.; Prenni, A. J.; Murray, B.; Wilson, M. A.; Tolbert, M. A. Infrared spectroscopic study of the deliquescence and efflorescence of ammonium sulfate aerosol as a function of temperature. *J. Geophys. Res.* **1999**, *104* (D17), 21317–21326.
- (22) Wise, M.; Biskos, G.; Martin, S.; Russell, L.; Buseck, P. Phase Transitions of Single Salt Particles Studied Using a Transmission Electron Microscope with an Environmental Cell. *Aerosol Sci. Technol.* **2005**, *39* (9), 849–856.
- (23) Laskina, O.; Morris, H. S.; Grandquist, J. R.; Estillore, A. D.; Stone, E. A.; Grassian, V. H.; Tivanski, A. V. Substrate-Deposited Sea Spray Aerosol Particles: Influence of Analytical Method, Substrate, and Storage Conditions on Particle Size, Phase, and Morphology. *Environ. Sci. Technol.* **2015**, *49* (22), 13447–13453.
- (24) Lee, C.; Sultana, C. M.; Collins, D. B.; Santander, M. V.; Axson, J. L.; Malfatti, F.; Cornwell, G. C.; Grandquist, J. R.; Deane, G. B.; Stokes, M. D.; Azam, F.; Grassian, V. H.; Prather, K. A. Advancing Model Systems for Fundamental Laboratory Studies of Sea Spray Aerosol Using the Microbial Loop. *J. Phys. Chem. A* **2015**, *119* (33), 8860–70.
- (25) (a) Leck, C.; Bigg, E. K. Biogenic particles in the surface microlayer and overlying atmosphere in the central Arctic Ocean during summer. *Tellus, Ser. B* **2005**, *57* (4), 2005. (b) Leck, C.; Bigg, E. K. Comparison of sources and nature of the tropical aerosol with the summer high Arctic aerosol. *Tellus, Ser. B* **2008**, *60* (1), 118–126. (c) Leck, C.; Bigg, E. K. Comparison of sources and nature of the tropical aerosol with the summer high Arctic aerosol. *Tellus, Ser. B* **2008**, *60* (1), 10.3402/tellusb.v60i1.16906. (d) Pósfai, M.; Li, J.; Anderson, J. R.; Buseck, P. R. Aerosol bacteria over the Southern Ocean during ACE-1. *Atmos. Res.* **2003**, *66* (4), 231–240.
- (26) Biller, S. J.; Schubotz, F.; Roggensack, S. E.; Thompson, A. W.; Summons, R. E.; Chisholm, S. W. Bacterial Vesicles in Marine Ecosystems. *Science* **2014**, *343* (6167), 183–186.
- (27) (a) Medronho, B.; Shafaei, S.; Szopko, R.; Miguel, M. G.; Olsson, U.; Schmidt, C. Shear-Induced Transitions between a Planar Lamellar Phase and Multilamellar Vesicles: Continuous versus Discontinuous Transformation. *Langmuir* **2008**, *24* (13), 6480–6486. (b) Guida, V. Thermodynamics and kinetics of vesicles formation processes. *Adv. Colloid Interface Sci.* **2010**, *161* (1–2), 77–88.
- (28) (a) Dobson, C. M.; Ellison, G. B.; Tuck, A. F.; Vaida, V. Atmospheric aerosols as prebiotic chemical reactors. *Proc. Natl. Acad. Sci. U. S. A.* **2000**, *97* (22), 11864–8. (b) Griffith, E. C.; Rapf, R. J.; Shoemaker, R. K.; Carpenter, B. K.; Vaida, V. Photoinitiated Synthesis of Self-Assembled Vesicles. *J. Am. Chem. Soc.* **2014**, *136* (10), 3784–3787.
- (29) Shiraiwa, M.; Zuend, A.; Bertram, A. K.; Seinfeld, J. H. Gas-particle partitioning of atmospheric aerosols: interplay of physical state, non-ideal mixing and morphology. *Phys. Chem. Phys.* **2013**, *15* (27), 11441–11453.
- (30) Ryder, O. S.; Campbell, N. R.; Shalowski, M.; Al-Mashat, H.; Nathanson, G. M.; Bertram, T. H. Role of Organics in Regulating ClNO₂ Production at the Air–Sea Interface. *J. Phys. Chem. A* **2015**, *119* (31), 8519–8526.
- (31) Chin, W.-C.; Orellana, M. V.; Verdugo, P. Spontaneous assembly of marine dissolved organic matter into polymer gels. *Nature (London, U. K.)* **1998**, *391* (6667), 568–571.
- (32) Alemán, J. V.; Chadwick, A. V.; He, J.; Hess, M.; Horie, K.; Jones, R. G.; Kratochvíl, P.; Meisel, I.; Mita, I.; Moad, G.; Penczek, S.; Stepto, R. F. T. Definitions of terms relating to the structure and processing of sols, gels, networks, and inorganic-organic hybrid materials (IUPAC Recommendations 2007). *Pure Appl. Chem.* **2007**, *79*, 1801.
- (33) Wurl, O. *Practical Guidelines for the Analysis of Seawater*; CRC Press: Boca Raton, FL, 2009.
- (34) (a) Verdugo, P. The role of marine gel-phase on carbon cycling in the ocean. *Mar. Chem.* **2004**, *92* (1–4), 65–66. (b) Verdugo, P.; Alldredge, A. L.; Azam, F.; Kirchman, D. L.; Passow, U.; Santschi, P. H. The oceanic gel phase: a bridge in the DOM-POM continuum. *Mar. Chem.* **2004**, *92* (1–4), 67–85. (c) Verdugo, P. Dynamics of marine biopolymer networks. *Polym. Bull. (Heidelberg, Ger.)* **2007**, *58* (1), 139–143. (d) Ding, Y.-X.; Chin, W.-C.; Verdugo, P. Development of a fluorescence quenching assay to measure the fraction of organic carbon present in self-assembled gels in seawater. *Mar. Chem.* **2007**, *106* (3–4), 456–462. (e) Cunliffe, M.; Murrell, J. C. The sea-surface microlayer is a gelatinous biofilm. *ISME J.* **2009**, *3* (9), 1001–1003. (f) Verdugo, P.; Santschi, P. H. Polymer dynamics of DOC networks and gel formation in seawater. *Deep Sea Res., Part II* **2010**, *57* (16),

1486–1493. (g) Radic, T. M.; Svetlicic, V.; Zutic, V.; Boulgaropoulos, B. Seawater at the nanoscale: marine gel imaged by atomic force microscopy. *J. Mol. Recognit.* **2011**, *24* (3), 397–405. (h) Verdugo, P. Marine microgels. *Ann. Rev. Mar. Sci.* **2012**, *4*, 375–400.

(35) Verdugo, P. Marine Microgels. *Annu. Rev. Mar. Sci.* **2012**, *4* (4), 375–400.

(36) Krysmann, M. J.; Castelletto, V.; Kelarakis, A.; Hamley, I. W.; Hule, R. A.; Pochan, D. J. Self-Assembly and Hydrogelation of an Amyloid Peptide Fragment. *Biochemistry* **2008**, *47* (16), 4597–4605.

(37) Verdugo, P. Marine Microgels. *Annu. Rev. Mar. Sci.* **2012**, *4* (4), 375–400.